[Frontiers in Bioscience 12, 1014-1023, January 1, 2007]

Oxygen delivery to the tissues and mitochondrial respiration

Dante L. Boveris and Alberto Boveris

Laboratory of Free Radical Biology, School of Pharmacy and Biochemistry, University of Buenos Aires, Buenos Aires, Argentina

TABLE OF CONTENTS

1. ABSTRACT

In mammals, the O_2 transport from the inspired air to the tissues is made by convective and diffusive mechanisms. The convective mechanisms are provided by the cardio-respiratory system and comprised by the basic variables of cardiac output and blood O_2 content. Microcirculation in arterioles and capillaries is adjusted to match the O_2 demand of local tissues. Endothelium-generated NO diffuses to the smooth muscle of microvessels and produces vasodilation that increases circulatory time in the capillaries and allows a more effective O_2 extraction in the tissues. Once within the tissue, O_2 diffuses to mitochondria where it is reduced in an exergonic process coupled to ATP synthesis. Both, O_2 and ATP are the two most homeostatic intracellular species. In heart and muscle, both species show unchanged levels with 25-100 times increases in work load and ATP turnover rate. The linear rates of O_2 uptake shown by tissue slices and perfused organs are interpreted as a fast switching of mitochondria between metabolic state 3 (with a fast rate of O_2 uptake and ATP synthesis) and state 4 (with a slow rate of O_2 uptake and no ADP phosphorylation). Endogenous mitochondrial NO, produced by mtNOS, sustains the concept of a physiological functional activity of this enzyme in regulating mitochondrial and cellular O_2 uptake.

2 . INTRODUCTION

During evolution, first bacteria and then eukaryotic cells and pluricellular organisms utilized molecular oxygen (O_2) in a process that was first catalyzed by enzymes of prokaryote plasma membrane and that evolved to be located into mitochondrial cristae. Mitochondria are intracellular organelles characterized by a high degree of genetic, metabolic and regulatory autonomy due to intracellular compartmentalization. The mitochondrial reduction of O_2 to water is coupled to the provision of a useful form of energy for cell works, through a highly efficient process that converts the chemical energy of the redox reactions into a H^+ electrochemical potential or proton-motive force that is then used to drive the endergonic synthesis of ATP. In the highly evolved mammals, the cellular steady state O_2 concentration is sustained by a convective mechanism powered by the cardio-respiratory system and by a diffusive mechanism that carries O_2 from the arteriolar and capillary bed to the cells. Diffusion is an entropy-driven process that dissipates O_2 gradients and that is effective only over short distances. Oxygen transport from lung alveoli to the red blood cells (RBC) in the capillaries surrounding the alveolar wall and from the RBC in the microvasculature to the tissues are diffusion-driven processes. The first model to describe O_2 exchange in a single capillary surrounded by a cylinder of

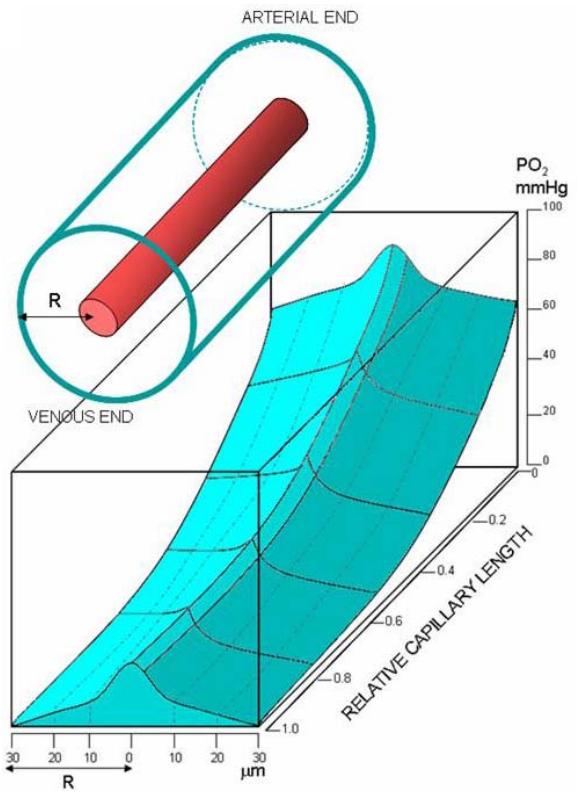

Figure 1. Scheme of the PO_2 according to the Krogh cylinder model. The blue surface indicates the PO_2 in a distance of up to 30 microns from the center of the O_2 carrying vessel. The mean PO_2 under normal conditions falls from 90 mmHg (12.0 kPa) at the arterial end of a capillary to 28 mmHg (3.7 kPa) at the venous end. Within a cross section of the cylinder-shaped tissue irrigated by the capillary, the mean PO_2 falls by 26 mmHg (3.5 kPa) from the capillary to the edge of the cylinder. Blood flow is 800 microl/g x min and O_2 consumption is 90 microl/g x min at 37°C. Redrawn from (2).

O_2-consuming tissue was formulated by Krogh (1) (Figure 1). The cylinder model has been since then the basis for most single-vessel models. Nowadays, systems containing multiple capillaries and vascular interactions allow large-scale simulations of complex microvascular networks (3)**.** On the basis of capillarity, cell shape and size, the intracellular pO_2 may differ considerably from one to another tissue and, considering different energy demands, for the same tissue under different physiological conditions (4).

3. METHODOLOGICAL DEFINITION OF VARIABLES

In the human body, O_2 transport from the heart to the tissues through the blood vessels is defined as O_2 delivery (DO_2, ml O_2/min), which is the product of cardiac output (C, l blood /min) and blood O_2 content, defined as the sum of the O_2 bound to Hb (HbO_2, ml O_2/l blood) and of the physically dissolved O_2 (S, ml O_2/l blood): $DO_2 = C \times (HbO_2 + S)$. The normal cardiac output (heart rate x stroke volume) in adult humans is about 5 l blood/min, a value that can be markedly increased by exercise and sympathetic regulation, yielding a normal DO_2 of about 1000 ml O_2 /min.

The maximal O_2-binding capacity of 1 g Hb (1.57 ml O_2) can be calculated (4 x 25.4/64,484) considering that 4 moles of O_2 (25.4 l O_2/mol at 37°C) bind reversibly to 1 mol of Hb (64,484 g). The contents of methemoglobin, the product of Hb oxidation that is unable to combine with O_2, and of carboxyhemoglobin account for 1-3 % of total Hb. The content of these species and other factors decrease the theoretical value to the maximal accepted physiological O_2-binding capacity of Hb: 1.34 ml O_2/g Hb at a pO_2 of 100 torr (1 torr = 1 mmHg) or 13.6 kPa at 37°C with 100% of Hb saturation ($SatO_2$). This value corresponds to 18.9 ml O_2/dl blood being transported by 14.5 g Hb/dl at 97.5% $SatO_2$, as it is the case in the lung.

The amount of physically dissolved O_2 (S) is pO_2- and temperature-dependent, with solubility being higher at lower temperatures and higher pO_2. The Henry O_2 solubility coefficient at 37°C is 0.0030 ml/dl x mmHg. At 21.3 kPa (the pO_2 of air at sea level) and 37°C, the solubility yields 185 microM O_2 in water (5) and the same value is taken for both plasma and blood. In the lung alveoli (13.6 kPa O_2 and 37°C), O_2 equilibrates with blood and yields an S value of 0.30 ml O_2/dl blood. Therefore, RBC and Hb that carry 18.9 ml O_2/dl blood afford most (98.4%) of the O_2 transported to the tissues. The round value of 20 ml O_2/dl arterial blood is frequently used, recognizing that Hb content is variable. In the microcirculation, the low O_2 carrying capacity of the plasma and the discrete flow of the RBC in capillaries account for fluctuations in capillary pO_2, that are named "erythrocyte-associated transients" of pO_2 (6). In cells and tissues, $[O_2]$ is in the range of 10-30 µM, that corresponds to a pO_2 of 8.6-25.8 torr or 1.15-3.45 kPa.

The whole O_2 consumption in the human body (VO_2) is calculated from the difference in O_2 content (HbO_2 + S) between the blood in the left atrium (arterial blood) and in the right atrium (venous blood). The normal O_2 content of venous blood is about 14.6 ml O_2 /dl as HbO_2 and 0.12 ml O_2/100 ml as S. The difference between arterial and venous blood, about 5.0 ml O_2/dl, accounts for the O_2 extraction in the tissues and corresponds to about 25% of the O_2 content of arterial blood. The concept of tissue O_2 extraction or O_2 extraction ratio (O_2ER), defined as the ratio between O_2 consumption (VO_2) and O_2 delivery (DO_2) as: $O_2ER = VO_2/DO_2$, is useful for organ considerations and for physiological and pathophysiological conditions as this value becomes independent of Hb content, $SatO_2$% and cardiac output.

If Hb were inexistent, the DO_2 (15 ml O_2/min) given by S (3 ml O_2/l blood) would only account for 6% of the basal VO_2 (about 250 ml O_2/min). If the pO_2 is elevated up to 3.0 atm in a hyperbaric chamber (303.9 kPa) while breathing pure O_2, S will be considerably increased to 45 ml O_2/l blood, thereby approaching DO_2 (225 ml O_2/min) to VO_2. Oxygen toxicity appears with hyperbaric O_2 after

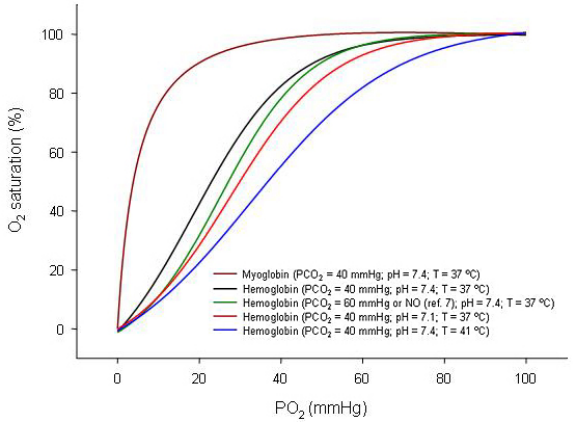

Figure 2. Hb/HbO_2 association/dissociation curves. The corresponding P_{50} values are: Mb/MbO_2=2.9 mmHg; Hb/HbO_2, 23 mmHg; Hb/HbO_2 and CO_2 or NO, 27 mmHg; Hb/HbO_2 and low pH, 30mmHg; Hb/HbO_2 and increased temperature, 36 mmHg.

hours of exposure, limiting its application to episodes of CO poisoning, gangrene and decompression sickness. Breathing the usual carbogen mixture (95% O_2 and 5% CO_2) at normal pressure provides a fully saturated Hb (1.34 ml O_2/g Hb) in the lung and 13.6 ml O_2/l blood as S.

In the microcirculation, RBC flux (RBC/s) is the product of RBC velocity (V, micron/s) and RBC lineal density (RBC/micron) as: RBC flux = V x LD. Oxygen flow in the capillaries (F_{O2}) is calculated with the RBC flux, the RBC-$SatO_2$ and the O_2 carrying capacity of a single RBC (B=0.0363 pl O_2/RBC at 100% $SatO_2$) as: F_{O2} = RBC flux × $SatO_2$% x B (7). Taking into account that most of the O_2 is not taken up by the tissues, capillary O_2 extraction ratio (O_2ERc) is calculated from capillary O_2 flow rates at the capillary entrance (in) and exit (out) as: $O_2ERc = [F_{O2}\ (in) - F_{O2}\ (out)] / F_{O2}\ (in)$. Changes in capillary O_2 extraction indicate localized mitochondrial or microvascular dysfunction.

4. CONVECTIVE TRANSPORT MECHANISMS

The Hb within erythrocytes is essential in the convective transport of O_2 by blood. The equilibrium between Hb and HbO_2 ($Hb + O_2 \Leftrightarrow HbO_2$) is not a simple chemical equilibrium characterized by an equilibrium constant. Instead, O_2 binds cooperatively with Hb, altering its tetrameric conformation and switching the O_2 binding properties. The process is adequately described by the HbO_2 and MbO_2 dissociation curves, in which the square hyperbola for MbO_2 shows a stiff high O_2 affinity (P_{50} = 2.9 mmHg) and the sigmoidal shape for HbO_2 shows a lower O_2 affinity (P_{50}= 23 mmHg) (2). P_{50} is the pO_2 necessary to half-saturate these O_2-binding proteins (Figure 2). The sigmoidal shape of the HbO_2 saturation/dissociation curve has fascinated scientists for a long time and fostered the concepts of cooperativity and changes in biochemical properties by protein conformation. In the tissues, the HbO_2 dissociation curve is shifted to the right, implying less affinity of Hb towards O_2, by the Bohr effect which is caused by the reversible combination of CO_2 to Hb protein amino groups after diffusion of CO_2 from the tissues to the RBC. The Bohr effect in arterioles and capillaries effectively improves tissue oxygenation and is also favored by the simultaneous decrease in pH and by changes in RBC metabolites, as 2,3-diphosphoglycerate (2). Other factors such as temperature increase or NO (8) also shift the curve to the right. It is important to emphasize that this rightward shift only occurs at a pO_2 below 60 torr (70 microM O_2, 8 kPa) which indicates a more effective O_2 supply to the tissues when metabolic stress, such as exercise or sepsis, takes place.

5. DIFFUSIVE TRANSPORT MECHANISMS

Oxygen diffusion is determined by Henry O_2 solubility (k), O_2 diffusivity (D), surface area through which exchange occurs (A), pO_2 gradient (delta pO_2) and length of the diffusion path (l) as established by Fick's law of diffusion (O_2 diffusion = -k x D x A x delta pO_2 / l). The critical O_2 diffusion distance, which is the maximum distance that mitochondria can be away from an O_2 source without anoxia and impaired function, is located at the edge of the Krogh [O_2] plot and ranges from 10 to hundreds of microns (9). This distance is determined by Fick O_2 diffusion parameters, which are rather constant, and capillary pO_2 and tissue O_2 consumption which are the two physiological variables.

An important observation is that the capillary-tissue contact area is only a fraction of the surface area of the inner mitochondrial membranes and cristae. By definition, this means that the highest gradients and highest O_2 fluxes are at the capillary-tissue cell interface and that these gradients are much shallower in the cytosol (10). Moreover, Mb further minimizes intracellular O_2 gradients in heart and muscle. It can be inferred that mitochondrial function is better served with a homeostatic and homogeneous intracellular O_2 steady-state concentration.

Once within the intracellular milieu, O_2 faces three independent factors: viscosity, binding and interference from cell structures, that account for the O_2 translational diffusion in the cytosol to be only 27% of the one in water (11). Viscosity in fibroblasts is 28% greater than in water, 19% of O_2 is transiently bound to low-mobility intracellular components and O_2 movement is hindered 2.5-fold by collisions with cell solids that comprise 13% of cell volume (11).

The diffusion of O_2 from arterioles to tissue was evaluated with a data acquisition system capable of obtaining values of microvessel diameter, RBC velocity, [Hb] and $SatO_2$% which allow O_2 convective flow to be calculated (see ref. 3 for equations and references therein). The calculated values indicate that most of the O_2 (about two-thirds) is released in the precapillary network and that the rate of diffusion is greater in small than in large arterioles, consistently with the lower velocity of blood in the smaller arterioles and their larger surface/volume ratio (12). Another interesting finding is that RBC gain O_2 as they pass through the capillaries near arterioles (13).

The half saturation of Mb with O_2 in cardiac and skeletal muscle occurs at a pO_2 of 2.9 mmHg or 3.3 microM O_2, which lies well below the tissue pO_2 of 10-25 mmHg or 12-30 microM O_2. Thus, under normal conditions Mb is in a largely oxygenated state acting as an O_2 reservoir and as a facilitator of O_2 diffusion favored by its random distribution in the citosol (14). Myoglobin knockout mice exhibit a slight but significant increase in blood Hb content (13.3 to 14.4 g/dl) and an identical Hb/hematocrit ratio indicating normal Hb content per RBC (15). Other functional adaptations in these mice include a significant (33%) increase of coronary blood flow, a higher maximal coronary flow elicited by 20 sec of coronary occlusion or 1 microM adenosine (both responses being elevated by 22%), and a 33% augmented capillary density in the heart (15). All these facts indicate an important role of Mb in O_2 delivery and in avoiding steep intracellular O_2 gradients in order to sustain a constant O_2 flow to the mitochondrial cristae.

Cold body temperatures, as experienced by many ectothermic animals either seasonally or chronically, produce physiological changes in O_2 delivery to the tissues (16). Taking 25°C as reference point and at atmospheric pressure, a decrease in temperature to 5°C increases O_2 solubility from 240 microM to 350 microM (5). The same temperature change produces a 70% increase in water viscosity affecting O_2 diffusion and the O_2 dissociation from MbO_2. However, the Mb and MbO_2 of Antarctic fishes exhibit convenient improvements of its association and dissociation constants (17). The mitochondrial compartment, *i.e.* the fraction of cytosol occupied by mitochondria, increases from 15% to 31% in the slow muscle fibers and from 2 % to 6 % in fast fibers in the acclimation of crucian carp from 28°C to 2°C, whereas the number of capillaries is augmented 2-fold (18). Results from striped bass muscle are similar: the cytosolic volume occupied by mitochondria increases from 29% to 45% in acclimation from 25°C to 5°C (19). Mitochondrial proliferation reduces the O_2 diffusion distance from capillaries to cristae, enhancing mitochondrial O_2 supply. Additionally, acclimation of striped bass from 25°C to 5°C increases intracellular neutral lipid droplets from 0.6% to 7.9% (19). An oil:water partition coefficient of 4.4 at 25°C indicates that lipid droplets act both as an O_2 reservoir and as low-resistance structures providing an 85% improvement in O_2 diffusion (20). Membranous conduits, a phenomenon seen in cold temperature fishes, improve O_2 delivery and provide an explanation of how mitochondria can obtain O_2 in the center of clusters (16). The epitome of cold adaptation is given by the Channichthydae, a family of hemoglobinless Antarctic fishes that also lack Mb in several genus (21).

6. REGULATION OF OXYGEN DELIVERY

Blood vessels controlling microcirculatory flow are understood as comprising flow-controlling vessels and distribution vessels. Most of the arterio-venous pressure gradient is dissipated in large flow-controlling vessels (medium-sized and large arterioles) that determine organ flow. On the other hand, the local tissue distribution of blood flow is determined downstream (small arterioles) by precapillary sphincters in tissues that have them or by similarly-sized precapillary arterioles in all tissues. Upstream, flow-controlling vessels are controlled by sympathetic tone and by regional neurohumoral systems. Conversely, distribution microvessels are under local control, responding to vasodilator metabolites (22). These metabolites produced by parenchymal cells under hypoxic conditions include adenosine (23), CO_2, NO, prostaglandins, lactate, H^+ and K^+ (22). Endothelial cells and smooth muscle cells respond to these stimuli to match vascular tone and O_2 delivery to increased local O_2 demand. The phenomenon is generally known as reactive hyperemia.

A Copernican revolution in microcirculatory physiology was produced with the identification of the EDRF (endothelium-derived relaxing factor) as NO. The endothelium-dependent vascular smooth muscle relaxation process was well characterized by 1982 and subsequent investigations recognized the involvement of cGMP and of nitric oxide synthases (NOS) (24). The discovery of the role of NO as a messenger in the cardiovascular system led to the 1998 Nobel Award in Physiology and Medicine to R. Furshgott, L. Ignarro and F. Murad.

Endothelial cells react to autonomic nervous system mediators (*i.e.* acetilcholine), to vasoactive substances (*i.e.* bradikynin and others), to intracellular Ca^{2+} signals and to vasodilator metabolites produced by parenchymal cells in hypoxic conditions with an activation of endothelial nitric oxide synthase (eNOS) (25). Nitric oxide diffuses from the endothelial cells to the adjacent smooth muscle cells, which respond to endothelium-derived NO with an stimulation of guanylate cyclase to produce cGMP, which in turn activates endoplasmic Ca^{2+} pump, reduces intracellular Ca^{2+} and dephosphorylates myosin light chains (26) (Figure 3). The described mechanism allows NO to play a crucial role in the regulation of whole body blood pressure. When L-NAME, a NOS blocker, is infused intravenously in rabbits or humans, it induces a raise in vascular resistance and blood pressure (27). This demonstrates that circulation resistance is in a constant state of vasodilation due to the continuous release of NO by the endothelium. It is to remark that NO was found involved in the response to shear stress in the rabbit heart as N-nitro-L-arginine (a NOS blocker) abolished completely the flow-dependent dilation (28). Also, hypoxic dilation was seen to be completely dependent on endothelium-derived NO in rat coronary small arteries as it was blocked by L-NAME or endothelium removal (29).

The molecular mechanism underlying reactive hyperemia is still largely unknown. However, it is known that beta-adrenoceptor-mediated vasodilation partially explains the exercise-induced hyperemia in the heart through its effect on large arteries and that alpha-adrenoceptor mediated vasoconstriction also protects subendocardial flow by increasing resistance in medium-sized intramyocardial vessels (30). An autonomic nervous system-mediated reactive hyperemia is a compelling

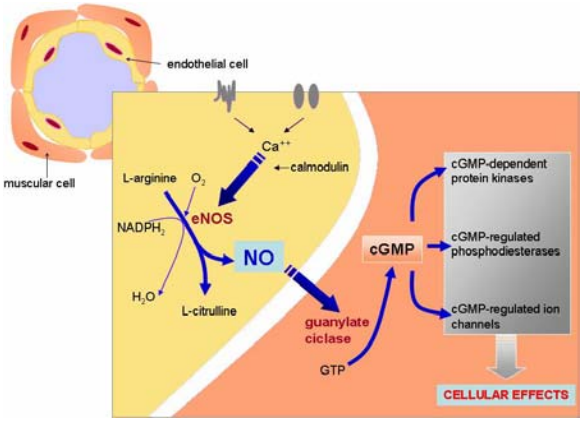

Figure 3. Scheme of the NO-cGMP signaling cascade in the microvesssels. The eNOS of the endothelial cells is activated by a rise in cellular [Ca^{2+}]. Nitric oxide diffuses to neighboring smooth muscle cells and activates guanylate cyclase that produces cGMP. The rise in intracellular cGMP levels in the target cell activates cGMP-dependent systems. The cGMP regulated ion channels include the Ca^{2+} pump of the sarcoplasmic reticulum. Redrawn from (24).

hypothesis because the same signal responsible for increasing VO_2 would simultaneously increase DO_2.

The nature of the reactive hyperemia vasodilatory signal in the microcirculation is proving to be difficult to elucidate. A gap-junction blocker, 18-beta-glycyrhetinic acid, failed to stop the propagation of the vasodilatory signal in capillaries, indicating that the electrotonic spread of membrane potential along the vessel wall is not involved. On the other hand, halothane and high osmolar sucrose did abolish the vasodilatory signal (31). Also, the transmitted signal is thought to be Ca^{2+}-independent as Fura-PE3, a Ca^{2+}-sensitive dye, failed to show intracellular Ca^{2+} changes in capillaries following increased muscle electrical stimulation (31). A fascinating answer, indeed complementary to the findings above, to the problem of the mediation of reactive hyperemia was given when an O_2 sensor was reported to exist in the erythrocyte itself. The pathway involves vasodilating ATP being released from RBC when sensing a low pO_2 and ATP acting on the endothelium to release NO (32).

A differential vascular reactivity should assure a rapid recruitment of vasodilatory mechanisms in the upstream direction. Whereas small arterioles (below 50 microns) show the greatest sensitivity to adenosine, myogenic mechanisms predominate in intermediate-sized arterioles (50-80 microns) and flow-dependent responses are mostly active in large arterioles (100 microns) (33). The myogenic response, defined as an intrinsic property of smooth muscle to respond to stretch or pressure, is effective in heart (34) and skeletal muscle (35) arterioles. It involves the endothelium-independent constriction of an arteriole following increases in intraluminal pressure and its dilation following decreases in intravascular pressure (36). In this manner, intermediate-sized vessels located upstream of the point of initial dilatation are able to respond to local pressure changes also dilating (because of a reduced intraluminal pressure) thus increasing the shear stress stimulus on large-sized arterioles and finally achieving their adaptation (vasodilatation) to a metabolism-induced elevation in flux. Intermediate-sized vessels, relying on this myogenic mechanism, are able to transmit the vasodilatory signal from small to large arterioles. The physiological relevance is evident when it is thought that large arterioles are the ones capable of maximal vasodilation (33,36).

Porcine subepicardial coronary arterial microvessels show 21%, 32% and 52% increases in diameter to maximal shear-stress in small (40 microns), intermediate (60 microns) and large arterioles (100 microns), respectively, whereas small arteries (180 microns) display only a 22% maximal dilation (36). The same pattern of differential vascular sensitivity was found when dose-response curves showed small arterioles to be more sensitive than larger arterioles and small arteries in the response to vasodilating substances such as adenosine or substance P. On the other hand, sodium nitroprusside (a NO donor) dose-response curves were identical in all vascular beds. These results suggest that segmental heterogeneity helps to coordinate the overall microvascular response during physiological stress and to optimize O_2 delivery to the tissues.

We will now focus on some VO_2/DO_2 considerations. As normal whole body DO_2 (1000 ml O_2/min) greatly surpasses basal VO_2 (250 ml O_2/min) a large DO_2 reserve enables the body to stay far from a DO_2 that implies hypoxia or anoxia, with VO_2 exhibiting a behavior largely independent of DO_2. Schlichtig *et al.* (37) have shown that when DO_2 is reduced below the critical point of 5.0 $\pm$ 0.8 ml/100 g x min in the liver, the VO_2 starts to decrease accordingly (Figure 4). Simultaneously, the beta-hydroxybutyrate/acetoacetate ratio (a measurement of the mitochondrial $NADH_2$/NAD ratio and by extension of mitochondrial redox state, was constant until a DO_2 value of 3.0 + 0.5 ml /100 g x min, being the difference statistically significant. At variance, kidney shows a 60% VO_2 reduction from its baseline value when it reaches the critical DO_2, indicating the inexistence of a supply-independent phase of O_2 consumption in this tissue (37). O_2ER was shown to be equally maximally elevated (0.86) when it reaches critical DO_2 values in the kidney and in whole body (38). In experiments in which DO_2 declines by progressive hemorrhage or by flow reduction, the VO_2 is physiologically protected by an increase in the O_2ER, presumably by recruitment of capillaries and autonomic-mediated blood flow redistribution (Figure 4). Thus, failure to achieve this increase in O_2ER during progressive DO_2 reductions is considered deleterious to the tissue, as it was observed after administration of deoxycholate or L-NAME and indomethacin that plundered endothelium vascular function (39). Adrenergic vasoconstriction, as indicated by the use of an alpha-adrenoreceptor antagonist (phenoxybenzamine), is also necessary to maintain efficiency in extracting O_2 during hypovolemic stress (40).

7. CELLULAR OXYGEN STEADY-STATE LEVELS

Constant and homeostatic O_2 levels in cells and tissues are the teleologic reason for the development and

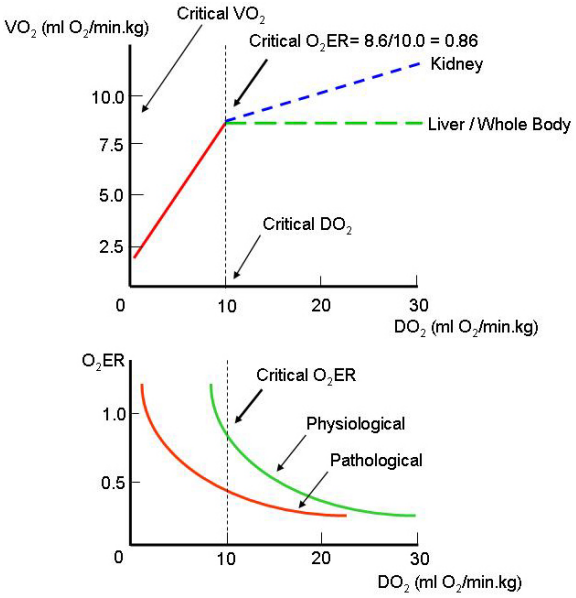

Figure 4. Relationships between oxygen delivery (DO_2), oxygen consumption (VO_2), and O_2 extraction ratio (O_2ER). Liver exhibits a supply-independent VO_2, whereas kidney does not. Pathological O_2ER is lower than physiological O_2ER due to mitochondrial dysfunction or because of an impairment in microvascular recruitment. Data from (36-38).

evolution of cardio-respiratory systems. In mammals, the range of usual [O_2] in tissues is 12-30 microM, considering dissolved O_2, or 10-25 mmHg or 1.3-3.3 kPa expressing the O_2 gas pressure in equilibrium with such O_2 concentration (5).

Intracelllular [O_2] and [ATP] are the most homeostatic cellular species, showing stable concentrations over a 100-fold ATP turnover rate, even though O_2 delivery correlates with the metabolic rate in a 1:1 fashion (41). In muscle and heart, where metabolic studies are thoughtful, O_2 uptake and ATP turnover are linearly related to the work rate (42). In these tissues, a randomly distributed MbO_2 contributes to eliminate O_2 gradients in the cytosol and the creatine phosphokinase reaction has a subsidiary role in maintaining a stable [ATP]. Phosphocreatine (descending) and phosphate (rising) changes, because of the creatine phosphokinase reaction, are also linear functions of work, but these changes are smaller (3-fold) compared with a 40-fold increased ATP turnover rate (43). Other pathways that supply ATP, such as glycolisis, the tricarboxylic acid cycle, amino acid metabolism and the beta-oxidation of fatty acid catabolism exhibit a modest (0.5- to 3-fold) increase in rates in the working tissue (41). This condition was described as "relatively" homeostatic because the relative changes in intermediate concentrations are far less than the percentage of the changes in metabolic rates with which they correlate. When 80% of aerobic maximum work rate in muscle and heart was sustained (the high metabolite rate was attainable because most of the cardiac output was available for muscle work), Mb oxygenation (70%) did not change with an ATP turnover rate of 80 micromol ATP/g tissue x min, 25 times increased over resting conditions (41).

At the gene level, adaptation to hypoxia involves the binding of the hypoxia-inducible factor-1 (HIF-1) to the hypoxia-responsive element of the regulated genes in a process understood to increase the expression of the proteins that increase O_2 delivery or that shallow cell and tissue O_2 gradients, enabling cells to survive in O_2 deficient conditions. About 40 hypoxia-inducible genes have been found to be regulated by HIF-1. Maduration of RBC, including iron transport and erythropoiesis, angiogenesis, vasomotor control, ATP metabolism and survival/death proteins are involved in this adaptation (44). It is worthy of note that in response to hypoxia the mitochondrial form of NOS, the mtNOS reacting with anti-iNOS antibodies (45), and the iNOS mRNA were found increased in cardiac myocites (46). The mRNA corresponding to iNOS was found increased in pulmonary artery endothelial cells (47), and the ones corresponding to nNOS and eNOS were also increased in the lung (48). It has been reported that NO concentrations over 1 microM stabilize HIF-1alpha, whereas lower levels, below 400 nM, prevent its accumulation (49). Moreover, HIF-1alpha stabilization and HIF-1 DNA binding activity were correlated with accumulation of NO_2 in the extracellular medium when iNOS expression was induced (49). It is then likely that hypoxia is associated with an increased NOS activity mediated by HIF-1alpha.

8. REGULATION OF MITOCHONDRIAL AND CELL RESPIRATION

Since the pioneering work by Chance & Williams (50,51) it has been known that ADP availability regulates mitochondrial and cellular O_2 uptake, based on the concepts of respiratory control and metabolic states. The former concept elegantly describes the state 4 to state 3 transition in which ADP regulates the rate of mitochondrial electron transfer and respiration (Figure 5). State 4, with availability of respiratory substrates but not of ADP and showing slow rates of O_2 uptake, was described as "controlled or resting respiration"; whereas state 3, with ample respiratory substrate and ADP availability was defined as the "active respiration", *i.e.* the maximal physiological rate of ATP production and O_2 consumption. In the transition from state 4 to state 3, after addition or availability of ADP, the rate of O_2 uptake is increased 3-10 times (51).

The linear rates of O_2 uptake observed in isolated tissues and perfused organs are interpreted as the result of a fast and random oscillation of mitochondria between states 3 and 4. This physiological condition, driven by local ATP demands, results in mitochondrial subpopulations exposed either to high ATP or ADP levels that decline or stimulate respiration (52,53).

The rates of O_2 uptake by isolated mitochondria in metabolic states 4 and 3, as well as the amount of mitochondrial protein per gram of organ and the O_2 uptake rates of the perfused organs for rat liver and heart are given in Table 1 (54). In the assumption that the whole tissue O_2

Table 1. Rates of the O_2 uptake in isolated mitochondria and in perfused rat liver and heart

	Oxygen uptake (nmol O_2/min x mg protein)[2]		**Content of mitochondria (protein/g organ)**	**Oxygen uptake of perfused organ (micromol O_2/min x g organ)**	**Fraction of mitochondria (%)**[3]	
	State 4	State 3			State 4	State 3
Rat liver[1]	10	88	32	1.4	57	43
Rat heart[1]	28	135	53	3.3[4]	68	32

[1] Temperature 30°C, [2] The rates of state 4 and 3 oxygen uptake were estimated for a substrate supply under physiological conditions: (3 x the rate with 5 mM malate and 5 mM glutamate as substrates) + (rate with 5 mM succinate as substrate)/4, [3] Fractions of mitochondria in state 4 and in state 3 calculated as indicated in equation [1] in the text, [4] Isolated beating heart, 280 beats/min.

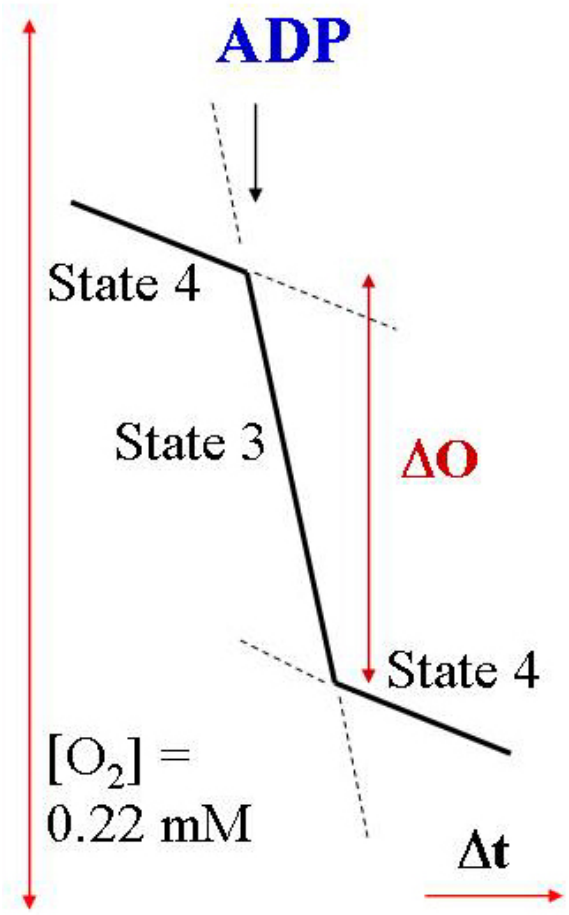

Figure 5. Scheme of the O_2 uptake by isolated mitochondria, as followed by a Clark-type O_2 electrode, that illustrates the respiratory control concept (50). State 4: mitochondrial metabolic state 4 in the presence of substrates, usually succinate or malate-glutamate. When the state 4 respiration after the expenditure of ADP (by phosphorylation to ATP) is faster than the initial state 4 respiration, it indicates mitochondrial uncoupling or excess Mg^{2+} in the reaction medium. State 3: mitochondrial metabolic state 3 after addition of ADP. The respiratory control is the ratio between the respiratory rates in state 4 and in state 3 (state 4/state 3; usually 3.0-7.0 with succinate and 4.0-10.0 with malate-glutamate). The amount of O atoms used to phosphorylate ADP under state 3 allows the estimation of oxidative phosphorylation energetic efficiency as the ADP:O ratio (usually 1.70 with succinate and 2.70 with malate-glutamate).

consumption is accounted for by the sum of the O_2 uptakes of mitochondria respiring in state 3 (a, in eq. [1]) and of mitochondria respiring in state 4 (1 – a, in eq. [1]), the fraction of mitochondria in states 3 and 4 under physiological conditions are estimated as 43% and 57% for rat liver and as 32% and 68% for rat heart.

Tissue O_2 consumption (O_2 uptake/min x g of tissue) = mitochondrial protein/g organ x [(a x state 3 rate O_2 uptake) + (1 – a) x (state 4 O_2 uptake)][1]

The reaction of reduced cytochrome oxidase, the O_2 acceptor and terminal enzyme of the mitochondrial respiratory chain, with O_2 is very fast ($k= 10^8/M^{-1}\ s^{-1}$) and the rate of electron transfer to cytochrome oxidase by the electron transfer chain is the key factor to define $K_{0.5}$, the operational O_2 concentration for half maximal rate of O_2 uptake, also named K_{MO2}. Evidence obtained by high resolution respirometry indicates $K_{0.5}$ values of 0.25-0.30 microM O_2 for state 4 mitochondria and 1.5-1.7 microM O_2 for state 3 mitochondria (55). The relative high value of $K_{0.5}$ is close enough to the physiological O_2 concentration to assume a critical dependence of mitochondrial respiration on tissue pO_2, understanding as critical pO_2 the one that by strict application of Michaelis-Menten kinetics will limit mitochondrial O_2 uptake below 80% of the maximal rate.

Valdez *et al.* (56) have recently introduced the concept of "mtNOS functional activity" to describe the effects of the NO generated by mtNOS in the regulation of mitochondrial O_2 uptake. Conditions of maximal NO levels (achieved by supplementation with arginine and superoxide dismutase) show diminished state 3 respiration rates whereas conditions of minimal NO levels (achieved by supplementation with NOS-blockers and Hb) show increased state 3 respiration rates. The difference in state 3 respiration (in the range of 15-65%) is named the mtNOS functional activity in the regulation of mitochondrial respiration (57). The mtNOS functional activity results much higher in state 3 than in state 4, in agreement with the kinetic characteristics of the NO inhibition of cytochrome oxidase (57). Considering that the NO produced by mtNOS is able to inhibit cytochrome oxidase activity by 22-25% in isolated heart and liver mitochondria (56), it can be calculated (equation [1]) that heart and liver mitochondria oscillate, about equally distributed, between a NO-inhibited state 3 (47% in heart and 58% in liver) and state 4 (53% in heart and 42% in liver). The NO-inhibited respiration lowers the steepness of intracellular O_2 gradients and allows O_2 to diffuse further along its gradient at the edge of

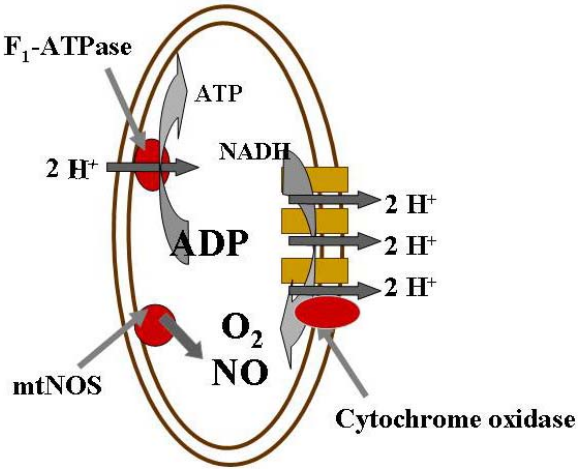

Figure 6. Regulation of mitochondrial respiration. Three mitochondrial proteins located in the inner membrane regulate the rate of electron transfer in the respiratory chain and mitochondrial and cellular O_2 uptake. 1. F_1-ATPase: dissipates the H^+ electrochemical gradient, or proton-motive force, coupled to ATP synthesis. The proton-motive force across the inner mitochondrial membrane is capable of decreasing electron transfer to the rate of state 4 respiration by matching the electrochemical potentials of the redox reactions and the proton-motive force. 2. mtNOS: the mitochondrial NOS isoenzyme produces NO that is a competitive inhibitor of cytochrome oxidase. 3. Cytochrome oxidase: the terminal oxidase of the mitochondrial respiratory chain whose activity is regulated by the ratio $[O_2]/[NO]$ (57).

Krogh's cylinder, extending the space of adequate tissue oxygenation away from the blood vessel (58, 59).

9. PERSPECTIVES

In summary, the rate of mitochondrial and cellular O_2 uptake and energy production in mammalian cells is regulated by energy demands (ADP level), O_2 supply and NO levels, this latter through the O_2/NO ratio. Three membrane-bound mitochondrial proteins, F_1-ATPase, mtNOS, and cytochrome oxidase are the regulable and operational effectors that regulate mitochondrial function based on the intramitochondrial ADP, NO and O_2 steady state concentrations (Figure 6).

10. ACKNOWLEDGEMENTS

This work was supported by grants B-075 from the University of Buenos Aires (UBA), PICT 00-8710 from *Agencia Nacional de Promoción Científica y Tecnológica* (ANPCYT) and PIP 2271-00 from *Consejo Nacional de Investigaciones Científicas y Técnicas* (CONICET), Argentina.

11. REFERENCES

1. Krogh A: The number and distribution of capillaries in muscles with calculations of the oxygen pressure head necessary for supplying the tissue. *J Physiol* 52, 409-415 (1919)

2. Grote J: Tissue respiration. In: Human Physiology. Eds: Schmidt, R. F. & G. Thews, Springer-Verlag, Berlin-Heidelberg-New York 510-522 (1983)

3. Pittman RN: Oxygen transport and exchange in the microcirculation. *Microcirculation* 12, 59-70 (2005)

4. Gayeski TEJ & C.R. Honig: Intracellular PO2 in individual cardiac myocytes in dogs, cats, rabbits, ferrets, and rats. *Am J Physiol* 260, 522-531 (1991)

5. Boveris A, L.E. Costa, E. Cadenas & J.J. Poderoso. Regulation of mitochondrial respiration by adenosine diphosphate, oxygen, and nitric oxide. *Meth Enzymol* 301, 188-198 (1999)

6. Golub AS & R.N. Pittman: Erythrocyte-associated transients in PO2 revealed in capillaries of rat mesentery. *Am J Physiol Heart Circ Physiol* 288, H2735-H2743 (2005)

7. Ellis CG, R.M. Bateman, M.D. Sharpe, W.J. Sibbald & R. Gill: Effect of a maldistribution of microvascular blood flow on capillary O_2 extraction in sepsis. *Am J Physiol Heart Circ Physiol* 282, H156-H164 (2002)

8. Kosaka H & A. Seiyama: Physiological role of nitric oxide as an enhancer of oxygen transfer from erythrocytes to tissues. *Biochem Biophy Res Commun* 218, 749-752 (1996)

9. Bateman RM, M.D. Sharpe & C.G. Ellis: Bench-to-bedside review: Microvascular dysfunction in sepsis: hemodynamics, oxygen transport, and nitric oxide. *Crit Care* 7, 359-373 (2003)

10. Honig CR, R.J. Connett & T.E. Gayeski: O2 transport and its interaction with metabolism; a systems view of aerobic capacity. *Med Sci Sports Exerc* 24, 47-53 (1992)

11. Kao HP, J.R. Abney & A.S. Verkman: Determinants of the translational mobility of a small solute in cell cytoplasm. *J Cell Biol* 120, 175-184 (1993)

12. Swain DP & R.N. Pittman: Oxygen exchange in the microcirculation of hamster retractor muscle. *Am J Physiol* 256, H247-H255 (1989)

13. Ellsworth ML & R.N. Pittman: Arterioles supply oxygen to capillaries by diffusion as well as by convection. *Am J Physiol* 258, H1240-H1243 (1990)

14. Wyman J: Facilitated diffusion and the possible role of myoglobin as a transport mechanism. *J Biol Chem* 241, 115-121 (1966)

15. Godecke A, U. Flogel, Z. Zanger, Z. Ding, J. Hirchenahin, U.K.M. Decking & J Schrader: Disruption of myoglobin in mice induces multiple compensatory

mechanisms. *Proc Natl Acad Sci USA* 96, 10495-10500 (1999)

16. Sidell BD: Intracellular oxygen diffusion: the roles of myoglobin and lipid at cold body temperature. *J Exp Biol* 201, 1118-1127 (1998)

17. Cashon RE, M.E. Vayda & B.D. Sidell: Kinetic characterization of myoglobins from vertebrates with vastly different body temperatures. *Comp Biochem Physiol* 117, 613-620 (1997)

18. Johnston IA: Capillarisation, oxygen diffusion distances and mitochondrial content of carp muscles following acclimation to summer and winter temperatures. *Cell Tissue Res* 222, 325-337 (1982)

19. Egginton S & Sidell B.D.: Thermal acclimation induces adaptive changes in subcellular structure of fish skeletal muscle. *Am J Physiol* 256, R1-R9 (1989)

20. Desaulniers N, T.S. Moerland & Sidell B.D.: High lipid content enhances the rate of oxygen diffusion through fish skeletal muscle. *Am J Physiol* 271, R42-R47 (1996)

21. Sidell BD, M.E. Vayda, D.J. Small, T.J. Moylan, R.L. Londraville, M.L. Yuan, K.J. Rodnick, Z.A. Eppley & L. Costello: Variable expression of myoglobin among the hemoglobinless Antarctic icefishes. *Proc Nac Acad Sci USA* 94, 3420-3424 (1997)

22. Vallet B: Vascular reactivity and tissue oxygenation. *Int Care Med* 24, 3-11 (1998)

23. Saito H, M. Nishimura, H. Shinano, H. Makita, I. Tsujino, E. Shibuya, F. Sato, K. Miyamoto & Y. Kawakami: Plasma concentration of adenosine during normoxia and moderate hypoxia in humans. *Am J Respir Crit Care Med* 159, 1014–1018 (1999)

24. Ignarro L: Introduction and overview. In: *Nitric Oxide: Biology and Pathobiology* (L. Ignarro, ed.). Academic Press, San Diego, 3-19 (2000)

25. Koesling D & A. Friebe: Structure-function relationships in guanylyl cyclase. In: *Nitric Oxide: Biology and Pathobiology* (L. Ignarro, ed.). Academic Press, San Diego 369-379 (2000)

26. Rapoport RM, M.B. Drazin & F. Murad: Endothelium-dependent relaxation in rat aorta may be mediated through cyclic GMP-dependent protein phosphorylation. *Nature* 306, 174-176 (1983)

27. Haynes WG, J.P. Noon, B.R. Walker & D.D. Webb: Inhibition of nitric oxide synthesis increases blood pressure in healthy humans. *J Hypertens* 11, 1375-1380 (1993)

28. Lamontagne D, U. Pohl & R. Busse: Mechanical deformation of vessel wall and shear stress determine the basal release of endothelium-derived relaxing factor in the intact rabbit coronary vascular bed. *Circ Res* 70, 123-130 (1992)

29. Lynch FM, C. Austin, A.M. Heagerty & A.S. Izzard: Adenosine and hypoxic dilation of rat coronary small arteries: roles of the ATP-sensitive potassium channel, endothelium and nitric oxide. *Am J Physiol Heart Circ Physiol* in press (2005)

30. Tune JD, M.W. Gorman & E.O. Feigl: Matching coronary blood flow to myocardial oxygen consumption. *J Appl Physiol* 97, 404-415 (2004)

31. Sarelius IH, K.D. Cohen & C.L. Murrant: Role for capillaries in coupling blood flow with metabolism. *Clin Exp Pharmacol Physiol* 27, 826-829 (2000)

32. Dietrich HH, M.L. Ellsworth, R.S. Sprague & R.G. Dacey Jr.: Red blood cell regulation of microvascular tone through adenosine triphosphate. *Am J Physiol Heart Circ Physiol* 278, H1294-H1298 (2000)

33. Jones CJH, L. Kuo, M.J. Davis & W.M. Chilian: Regulation of coronary blood flow: coordination of heterogeneous control mechanisms in vascular microdomains. *Cardiovasc Res* 29, 585-596 (1995)

34. Kuo L, W. Chilian & M.J. Davis: Coronary arteriolar myogenic response is independent of endothelium. *Circ Res* 66, 860-866 (1990)

35. Falcone JC, M.J. Davis & G.A. Meininger: Endothelium independence of the myogenic response in isolated skeletal muscle arterioles. *Am J Physiol* 26, H130-H135 (1991)

36. Kuo L, M.J. Davis & W.M. Chillian: Longitudinal gradients for endothelium-dependent and -independent vascular responses in the coronary microcirculation. *Circulation* 92, 518-525 (1995)

37. Schlichtig R, H.A. Klions, D.J. Kramer & E.M. Nemoto: Hepatic dysoxia commences during O2 supply dependence. *J Appl Physiol* 72, 1499-1505 (1992)

38. Schlichtig R, D.J. Kramer, J.R. Boston & M.R. Pinsky: Renal O2 consumption during progressive hemorrhage. *J Appl Physiol* 70, 1957-1962 (1991)

39. Curtis SE, B. Vallet, M.J. Winn, J.B. Caufield, C.E. King, C.K. Chapler & S.M. Cain: Role of the vascular endothelium in O2 extraction during progressive ischemia in canine skeletal muscle. *J Appl Physiol* 79, 1351-1360 (1995)

40. Maginnis LA, H. Connolly, R.W. Samsel & P.T. Schumacker: Adrenergic vasoconstriction augments tissue O_2 extraction during reductions in O_2 delivery. *J Appl Physiol* 76, 1454-1461 (1994)

41. Hochachka PW: The metabolic implications of intracellular circulation. *Proc Natl Acad Sci USA* 96, 12233-12239 (1999)

42. Andersen P & B. Saltin: Maximal persfusion of skeletal muscle in man. *J Physiol* 366, 233-249 (1985)

43. Allen PS, G.O. Matheson, G. Zhu, D. Gheorgiu, R.S. Dunlop, T. Falconer, C. Stanley & P.W. Hochachka: Simultaneous 31P magnetic resource spectroscopy of the soleus and gastrocnemius in Sherpas during graded calf muscle exercise and recovery. *Am J Physiol* 272, R999-R1007 (1997)

44. Zagórska A & J. Dulak: HIF-1: the knowns and unknowns of hypoxia sensing. *Acta Biochim Polon* 51, 563-585 (2004)

45. Gonzalez GF, F.A. Chung, S. Miranda, L.B. Valdez, T. Zaobornyj & A. Boveris: Heart mitochondrial nitric oxide synthase is upregulated in male rats exposed to high altitude (4340 m). *Am J Physiol Heart* 288: 2568-2573 (2005)

46. Jung F, L.A. Palmer, N. Zhou & R.A. Johns: Hypoxic regulation of inducible nitric oxide synthase via hypoxia inducible factor-1 in cardiac myocytes. *Circ Res* 86, 319-325 (2000)

47. Palmer LA, G.L. Semenza, M.H. Stoler & R.A. Johns: Hypoxia induces type II NOS gene expression in pulmonary artery endothelial cells via HIF-1. *Am J Physiol* 274, L212-L219 (1998)

48. Shaul PW, A.J. North, T.S. Brannon, K. Ujiie, L.B. Wells, P.A. Nisen, C.J. Lowenstein, S.H. Snyder & R.A. Star: Prolonged *in vivo* hypoxia enhances nitric oxide synthase type I and type III gene expression in adult rat lung. *Am J Respir Cell Mol Biol* 13, 167-174 (1995)

49. Mateo J, M. García-Lecea, S. Cadenas, C. Hernández & S. Moncada: Regulation of hypoxia-inducible factor-1alpha by nitric oxide through mitochondria-dependent and -independent pathways. *Biochem J* 376, 537–544 (2003)

50. Chance B & G.R. Williams: A simple and rapid assay of oxidative phosphorylation. *Nature* 175, 1120-1121 (1955)

51. Chance B & G.R. Williams: Respiratory enzymes in oxidative phosphorylation. I. Kinetics of oxygen utilization. *J Biol Chem* 217, 383-393 (1955)

52. Shiva S, J.Y. Oh, A.L. Landar, E. Ulasova, A. Venkatraman, S.M. Bailey & V.M. Darley Usmar: Nitroxia: the pathological consequence of dysfunction in the nitric oxide-cytochrome c oxidase signaling pathway. *Free Radic Biol Med* 38, 297-306 (2005)

53. Navarro A, R. Torrejon, M.J. Bandez, J.M. Lopez-Cepero & A. Boveris: Mitochondrial function and mitochondria-induced apoptosis in an overstimulated rat ovarian cycle. *Am J Physiol Endocrinol Metab* 289, E1101-E1110 (2005)

54. Boveris A, L.E. Costa & E. Cadenas: The mitochondrial production of oxygen radicals and cellular aging. In: Understanding the process of aging. Eds.: E. Cadenas, L. Packer. Marcel Dekker, Inc., New York 1-16 (1999)

55. Costa LE, G. Mendez & A. Boveris: Oxygen dependence of mitochondrial function measured by high-resolution respirometry in long-term hypoxic rats. *Am J Physiol* 273, 852-858 (1997)

56. Valdez LB, T. Zaobornyj & A. Boveris: Functional activity of mitochondrial nitric oxide synthase. *Meth Enzymol* 396: 444-455 (2005)

57. Antunes F, A. Boveris & E. Cadenas: On the mechanism and biology of cytochrome oxidase inhibition by nitric oxide. *Proc Natl Acad Sci USA* 101, 16774-16779 (2004)

58. Poderoso JJ, M.C. Carreras, C. Lisdero, N. Riobo, F. Schopfer & A. Boveris: Nitric oxide inhibits electron transfer and increases superoxide radical production in rat heart mitochondria and submitochondrial particles. *Arch Biochem Biophys* 328, 85-92 (1996)

59. Thomas DD, X. Liu, S.P. Kantrow & J.R. Lancaster Jr.: The biological lifetime of nitric oxide: implications for the perivascular dynamics of NO and O2. *Proc Natl Acad Sci USA* 98, 355-360 (2001)

Abbreviations: Hb: hemoglobin; Mb: myoglobin; HbO_2: oxyhemoglobin; MbO_2: oxymyoglobin

Key Words: oxygen uptake, oxygen diffusion; mtNOS functional activity; NO-mediated vasodilation; hyperemia; homeostatic oxygen levels, Review

Send correspondence to: Professor Alberto Boveris, Laboratory of Free Radical Biology, Junin 956, School of Pharmacy and Biochemistry, University of Buenos Aires, C1113AAD Buenos Aires, Argentina, Tel: 541145083646, Fax: 54-11-4508-3646 Ext. 102, E-mail: aboveris@ffyb.uba.ar

http://www.bioscience.org/current/vol12.htm